WSI
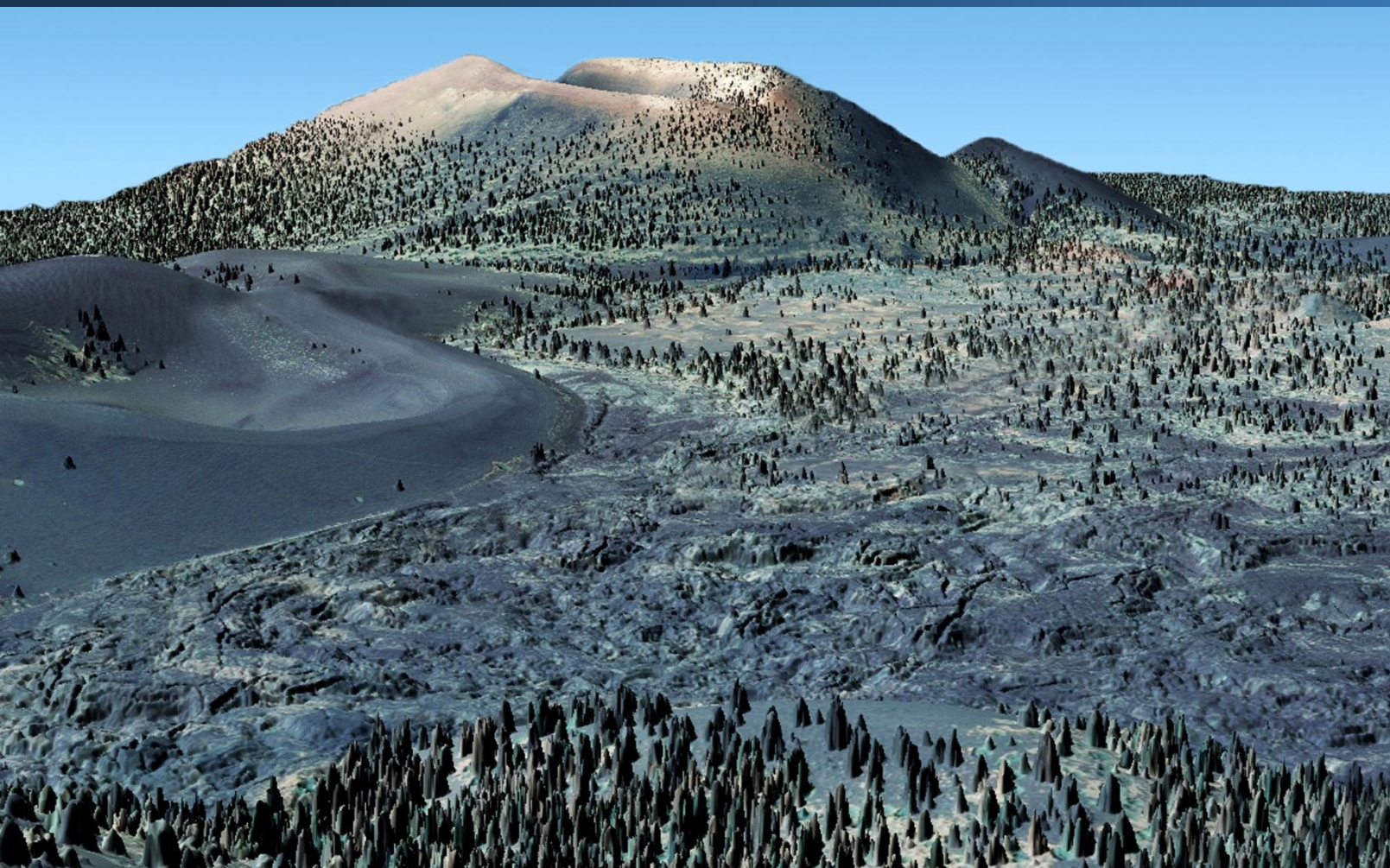
Applied
Remote Sensing
and Analysis

# Sunset Crater LiDAR

Technical Data Report

WSI

Paul Whitefield
Flagstaff Area National Monuments
6400 N. Highway 89
Flagstaff, AZ 86004
PH: 928-526-1157 ext. 235

WSI Corvallis Office
517 SW 2nd St., Suite 400
Corvallis, OR 97333
PH: 541-752-1204

# TABLE OF CONTENTS

**Cover Photo:** View looking Southeast over the lava flow at Sunset Crater Volcano National Monument. Image derived from all LiDAR points colored by 2010 NAIP imagery.

View of the Sunset Crater
LiDAR site in Arizona ▶

In August 2012, WSI (Watershed Sciences, Inc.) was contracted by the USDOI National Parks Service (NPS) to collect Light Detection and Ranging (LiDAR) data and digital imagery in the fall of 2012 for the Sunset Crater Volcano National Monument site in Arizona (Figure 1). Data were collected to aid the NPS in monitoring unique topographic and geophysical properties of the study area.

The following report accompanies the delivered LiDAR data documenting the data acquisition, processing methods, and results of accuracy assessments. Project summary details are provided below (Table 1), including contracted deliverables provided to NPS (Table 2).

**Table 1: Acquisition dates, acreages, and data types collected on the Sunset Crater LiDAR site.**

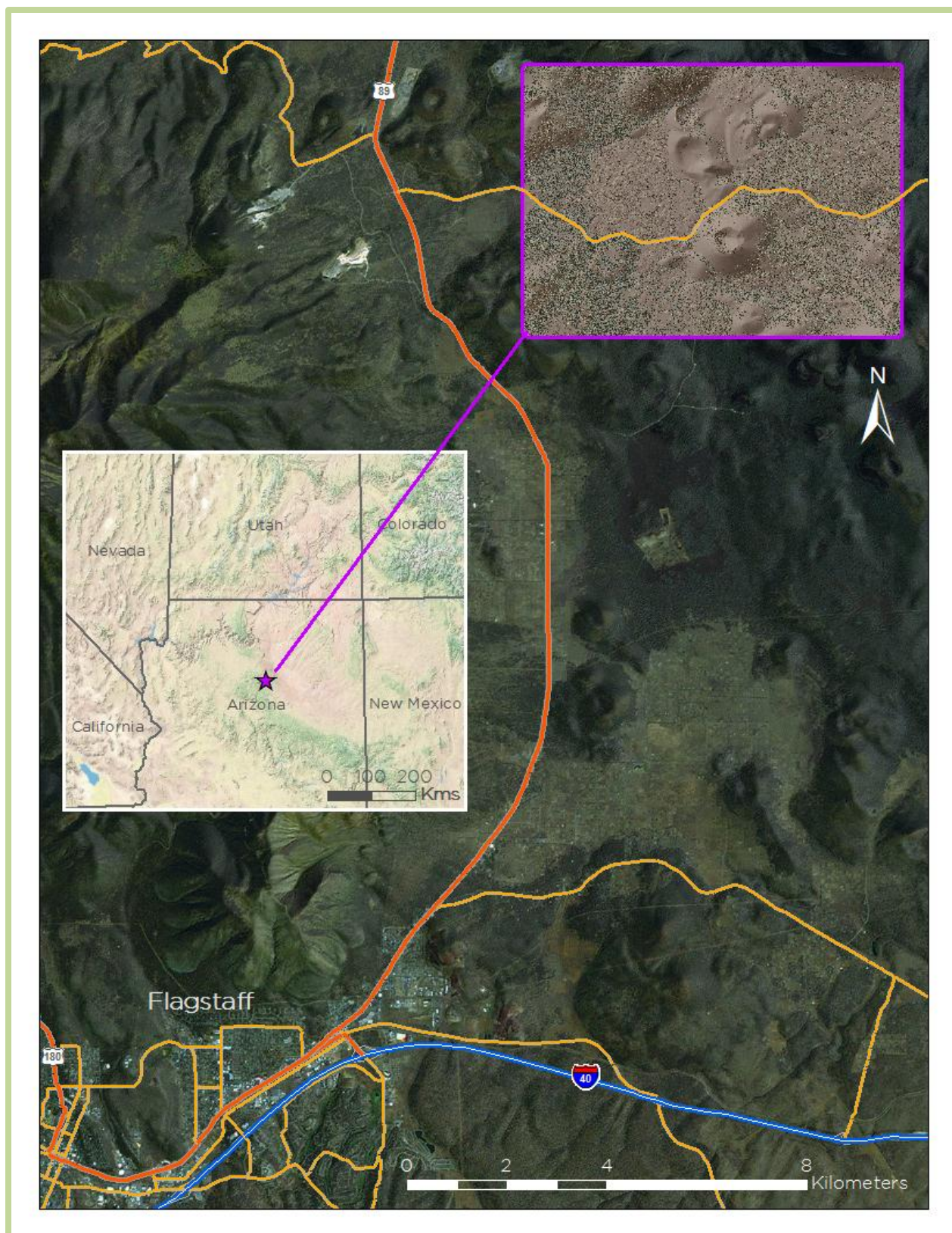| Project Site | Contracted Acres | Buffered Acres | Acquisition Dates | Data Type |
|---|---|---|---|---|
| Sunset Crater | 9,600 | 10,233 | 09/16/2012 | LiDAR |

Figure 1: Location map of the Sunset Crater LiDAR site near Flagstaff, Arizona

**Table 2: Products delivered to NPS for the Sunset Crater LiDAR site**

| Sunset Crater LiDAR Products Projection: UTM Zone 12 North Horizontal Datum: NAD83 (CORS96) Vertical Datum: NAVD88 (GEOID09) Units: Meters | |
| --- | --- |
| LAS Files | LAS v 1.2 <br> • All Returns |
| Rasters | 1 Meter ESRI Grids and GeoTiffs <br> • Bare Earth Model <br> • Highest Hit Model <br> 0.5 Meter GeoTiffs <br> • Intensity Images |
| Vectors | Shapefiles (.shp) <br> • Site Boundary <br> • LiDAR Index <br> • DEM/DSM Index <br> • RTK Check Points <br> • Land Cover Check Points |

Trimble R7 survey setup at the
Sunset Crater LiDAR site ▶

# Planning

In preparation for data collection, WSI reviewed the project area using Google Earth, and flightlines were developed using ALTM-NAV Planner (v.3.0) software. Careful planning entailed adapting the pulse rate, flight altitude and ground speed in order to ensure complete coverage of the Sunset Crater LiDAR study area at the target point density of ≥8 pulses per square meter, while optimizing flight paths to minimize flight times. This process entails preparing for known factors such as satellite constellation availability and weather windows. In addition, a variety of logistical considerations require review: private property access, potential air space restrictions and availability of company resources (both staff and equipment). Any weather hazards and conditions affecting the flight were continuously monitored due to their impact on the daily success of airborne and ground operations.

# Ground Survey

Geo-spatial correction of the aircraft positional coordinate data and quality assurance checks on final LiDAR data and orthoimagery products require quality ground survey data. Permanent survey monuments and real time kinematic (RTK) surveys typically assist the LiDAR acquisition process.



## Monumentation

The spatial configuration of ground survey monuments provided redundant control within 13 nautical miles of the mission areas for LiDAR flights. Monuments were also used for collection of ground control points using real time kinematic (RTK) survey techniques (see section **RTK** below).

Monument locations were selected with consideration for satellite visibility, field crew safety, and optimal location for RTK coverage. WSI utilized one existing control point and established one new monument for the Sunset Crater LiDAR project (Table 3, Figure 3). The existing monument was a well cap (Figure 2) designated for use within the project area. New monumentation was set using 5/8" rebar topped with stamped 2" aluminum caps.

**Table 3: Monuments established for the Sunset Crater LiDAR acquisition. Coordinates are on the NAD83 (CORS96) datum, epoch 2002**

| Monument ID | Latitude | Longitude | Ellipsoid (meters) |
|---|---|---|---|
| WELLCAP | 35° 22' 14.75264" | -111° 32' 48.97863" | 2088.261 |
| SC_LIDAR | 35° 22' 17.33901" | -111° 29' 24.10660" | 2129.761 |

To correct the continuous onboard measurements of the aircraft position recorded throughout the missions, WSI concurrently conducted multiple static Global Navigation Satellite System (GNSS) ground surveys (1 Hz recording frequency) over each monument. After the airborne survey, the static GPS data were triangulated with nearby Continuously Operating Reference Stations (CORS) using the Online Positioning User Service (OPUS1) for precise positioning. Multiple independent sessions over the same monument were processed to confirm antenna height measurements and to refine position accuracy. All static surveys were collected with Trimble model R7 GNSS receivers equipped with a Zephyr Geodetic Model 2 RoHS antenna. All GNSS measurements were made with dual frequency L1-L2 receivers with carrier-phase correction.

[1] OPUS is a free service provided by the National Geodetic Survey to process corrected monument positions. http://www.ngs.noaa.gov/OPUS.

# RTK

For the RTK check point data collection, a Trimble R7 base unit was positioned at a nearby monument to broadcast a kinematic correction to a roving Trimble R8 GNSS receiver. All RTK measurements were made during periods with a Position Dilution of Precision (PDOP) of ≤ 3.0 with at least six satellites in view of the stationary and roving receivers. When collecting RTK points, the rover would record data while stationary for five seconds, then calculate the pseudorange position using at least three one-second epochs. Relative errors for the position must be less than 1.5 cm horizontal and 2 cm vertical in order to be accepted. Table 4 summarizes the specifications for the Trimble R7 and R8 units.

Table 4: Trimble equipment identification

| Receiver Model | Antenna | OPUS Antenna ID | Use |
|---|---|---|---|
| Trimble R7 GNSS | Zephyr GNSS Geodetic Model 2 | TRM57971.00 | Static |
| Trimble R8 | Integrated Antenna R8 Model 2 | TRM_R8_GNSS | RTK |

RTK positions were collected on hard surface locations such as gravel or stable dirt roads that also had good satellite visibility. RTK measurements were not taken on highly reflective surfaces such as center line stripes or lane markings on roads. The distribution of RTK points depended on ground access constraints, and may not be equitably distributed throughout the study area. See Figure 3 for the distribution of RTK in this project.



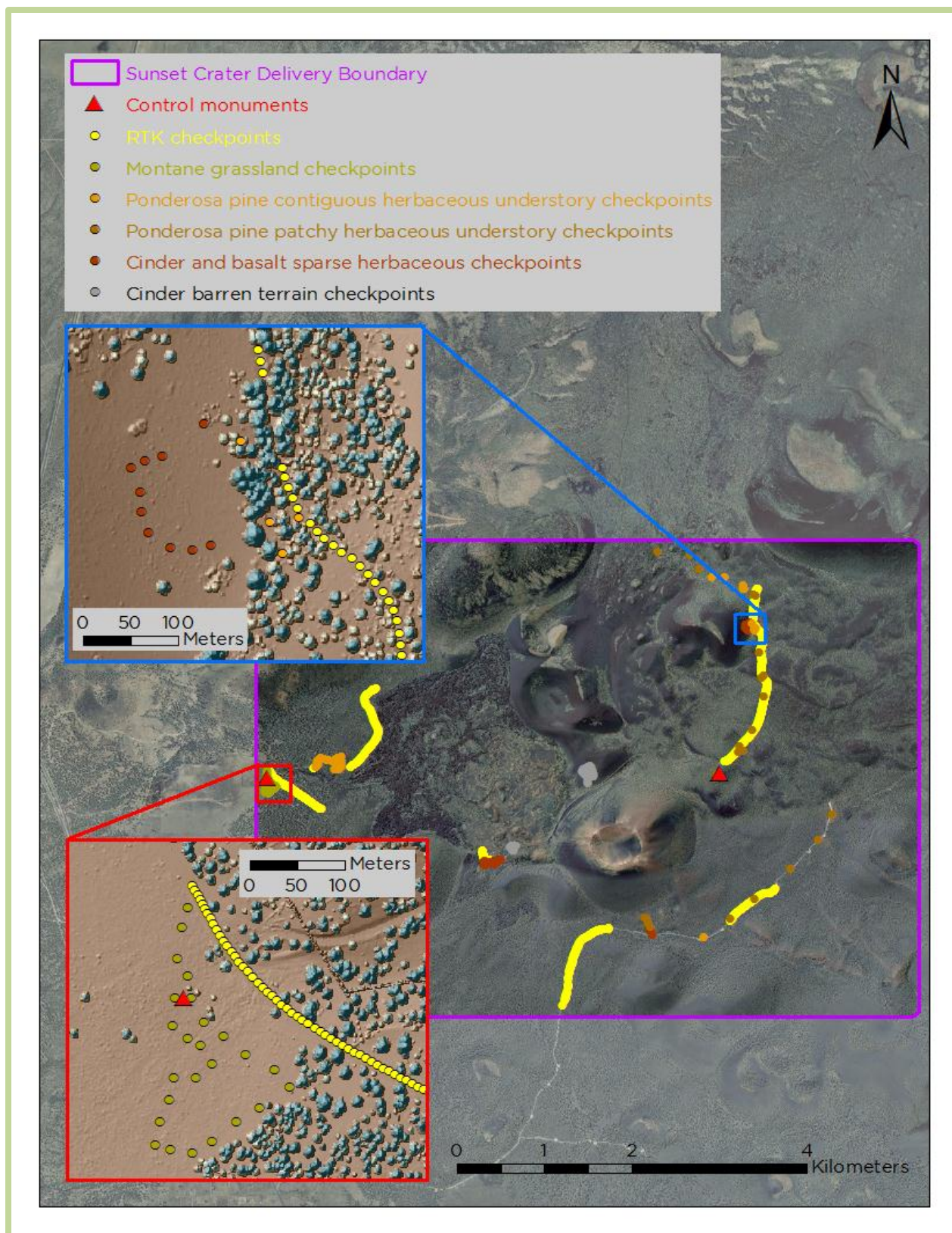Figure 2: Wellcap monument used for the LiDAR acquisition at the request of the NPS.

Figure 3: Basestation, RTK, and land cover checkpoints in the Sunset Crater AOI

# Land Cover

In addition to control point RTK, land cover check points were taken throughout the study area. Land cover types and descriptions can be referenced in Table 5. Individual accuracies were calculated for each land-cover type to assess confidence in the LiDAR derived ground models across land cover classes.

**Table 5: Land cover descriptions of check points taken for the Sunset Crater AOI**

| Land cover type | Land cover code | Example | Description |
|---|---|---|---|
| Montane grassland | MG |  | Montane grassland |
| Ponderosa Pine (contiguous) | CONTIG |  | Ponderosa pine with continuous shrub herbaceous understory and needle cast |
| Ponderosa Pine (patchy) | PATCHY |  | Ponderosa pine with patchy shrub herbaceous understory and needle cast |
| Cinder and Basalt (sparse herbaceous) | CB |  | Cinder and basalt sparse herbaceous shrubland |
| Cinder terrain | CT |  | Cinder barren terrain |

# Airborne Survey

## LiDAR

The LiDAR survey was accomplished with a Leica ALS50 Phase II mounted in a Cessna Caravan. Table 6 summarizes the settings used to yield an average pulse density of ≥8 pulses/m$^2$ over the Sunset Crater LiDAR terrain. It is not uncommon for some types of surfaces (e.g. dense vegetation or water) to return fewer pulses than the laser originally emitted. These discrepancies between native and delivered density will vary depending on terrain, land cover, and the prevalence of water bodies.

Table 6: LiDAR survey settings and specifications for the Sunset Crater LiDAR site

| LiDAR Survey Settings & Specifications | |
| --- | --- |
| Sensor | ALS 50 |
| Survey Altitude (AGL) | 900 m |
| Target Pulse Rate | 106 kHz |
| Sensor Configuration | Single Pulse in Air (SPIA) |
| Laser Pulse Diameter | 21 cm |
| Mirror Scan Rate | 66.3 Hz |
| Field of View | 26$^0$ |
| GPS Baselines | ≤13 nm |
| GPS PDOP | ≤3.2 |
| GPS Satellite Constellation | ≥6 |
| Maximum Returns | 4 |
| Intensity | 8-bit |
| Resolution/Density | Average 8 pulses/m$^2$ |
| Accuracy | RMSE$_Z$ ≤ 15 cm |

All areas were surveyed with an opposing flight line side-lap of ≥50% (≥100% overlap) to reduce laser shadowing and increase surface laser painting. The Leica laser systems record up to four range measurements (returns) per pulse. All discernible laser returns were processed for the output dataset.

To accurately solve for laser point position (geographic coordinates x, y, z), the positional coordinates of the airborne sensor and the attitude of the aircraft were recorded continuously throughout the LiDAR data collection mission. Position of the aircraft was measured twice per second (2 Hz) by an onboard differential GPS unit. Aircraft attitude was measured 200 times per second (200 Hz) as pitch, roll, and yaw (heading) from an onboard inertial measurement unit (IMU). To allow for post-processing correction and calibration, aircraft/ sensor position and attitude data are indexed by GPS time.

3D point cloud of looking southeast at part of the Bonito lava flow at the base of the Sunset Crater ▶
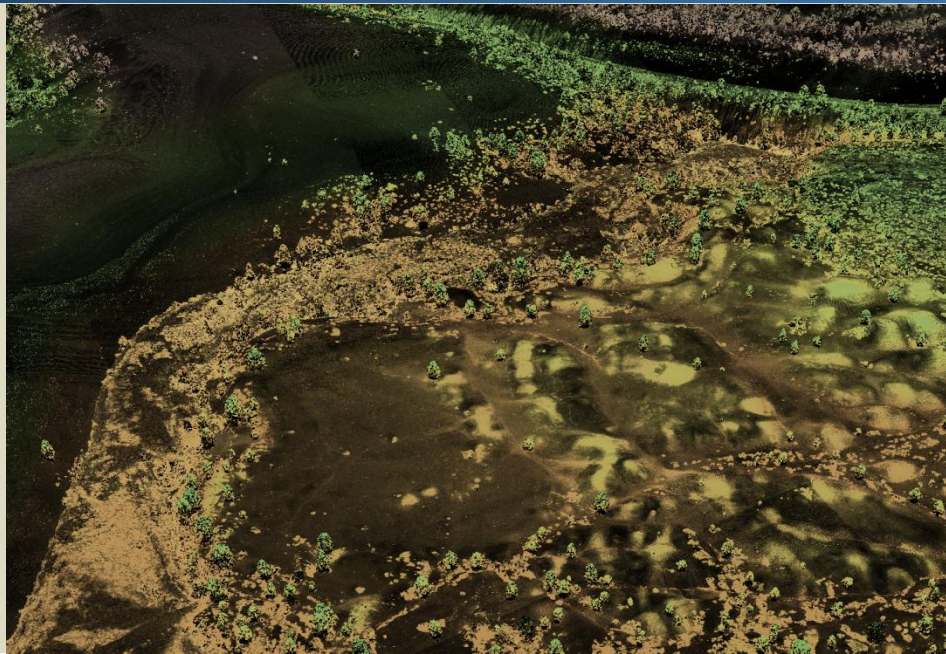
# LiDAR Data

Upon the LiDAR data's arrival to the office, WSI processing staff initiated a suite of automated and manual techniques to process the data into the requested deliverables. Processing tasks included GPS control computations, kinematic corrections, calculation of laser point position, calibration for optimal relative and absolute accuracy, and classification of ground and non-ground points (Table 7). A full description of these tasks can be found in Table 8.

**Table 7: ASPRS LAS classification standards applied to the Sunset Crater dataset.**

| Classification Identification Number | Classification Name | Classification Description |
|---|---|---|
| 1 | Default/ Unclassified | Laser returns that are not included in the ground class and not dismissed as Noise or Withheld points. |
| 2 | Ground | Ground that is determined by a number of automated and manual cleaning algorithms to determine the best ground model the data can support. |
| 7 | Noise | Laser returns that are often associated with birds or artificial points below the ground surface "pits". |
| 11 | Withheld | Laser returns that have intensity values of 0 or 255. |

**Table 8: LiDAR processing workflow**

| LiDAR Processing Step | Software Used |
|---|---|
| Resolve kinematic corrections for aircraft position data using kinematic aircraft GPS and static ground GPS data. | Waypoint GPS v.8.3 Trimble Business Center v.2.80 Blue Marble Desktop v.2.5 |
| Develop a smoothed best estimate of trajectory (SBET) file that blends post-processed aircraft position with attitude data. Sensor head position and attitude are calculated throughout the survey. The SBET data are used extensively for laser point processing. | IPAS TC v.3.1 |
| Calculate laser point position by associating SBET position to each laser point return time, scan angle, intensity, etc. Create raw laser point cloud data for the entire survey in *.las (ASPRS v. 1.2) format. Data are converted to orthometric elevations (NAVD88) by applying a Geoid03 correction. | ALS Post Processing Software v.2.74 |
| Import raw laser points into manageable blocks (less than 500 MB) to perform manual relative accuracy calibration and filter erroneous points. Ground points are then classified for individual flight lines (to be used for relative accuracy testing and calibration). | TerraScan v.12.004 |
| Using ground classified points per each flight line, the relative accuracy is tested. Automated line-to-line calibrations are then performed for system attitude parameters (pitch, roll, heading), mirror flex (scale) and GPS/IMU drift. Calibrations are performed on ground classified points from paired flight lines. Every flight line is used for relative accuracy calibration. | TerraMatch v.12.001 |
| Import position and attitude data. Classify resulting data as ground and non-ground points. Assess statistical absolute accuracy via direct comparisons of ground classified points to ground RTK survey data. | TerraScan v.12.004 TerraModeler v.12.002 |
| Generate bare earth models as triangulated surfaces, export as ArcInfo ASCII grids at 1 meter pixel resolution, and mosaic as ESRI grids. Also export ASCII grids of the first return point surface at 1 meter pixel resolution to generate highest hit models. | TerraScan v.12.004 ArcMap v. 10.0 TerraModeler v.12.002 |

Bare earth image of Sunset Crater colored by elevation ▶
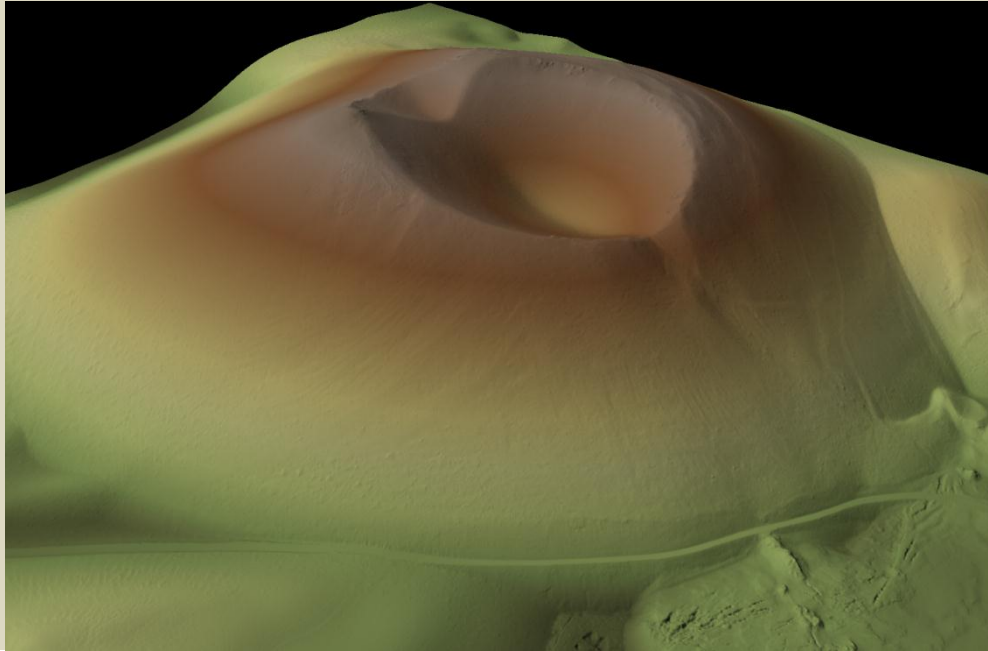


# LiDAR Density

The average first-return density for the LiDAR data was 12.80 points/m$^2$ (Table 9). The pulse density distribution will vary within the study area due to laser scan pattern and flight conditions. Additionally, some types of surfaces, such as breaks in terrain, water, and steep slopes, may return fewer pulses (delivered density) than originally emitted by the laser (native density).

The statistical distribution of first returns (Figure 4) and classified ground points (Figure 5) are portrayed below. Also presented are the spatial distribution of average first return densities (Figure 6) and ground point densities (Figure 7) for each 100 m$^2$ cell.

**Table 9: Average LiDAR point densities**

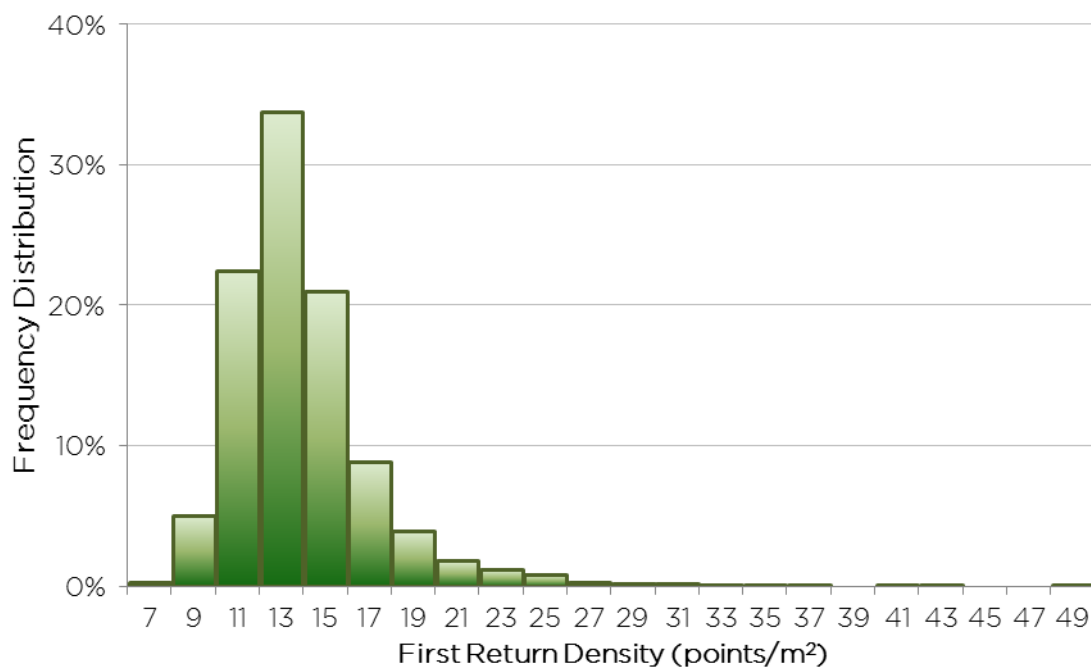| Classification | Point Density |
|---|---|
| First-Return | 12.80 points/m$^2$ |
| Ground Classified | 5.89 points/m$^2$ |

**Figure 4: Frequency distribution of first return densities (native densities) of the 1m gridded study area**
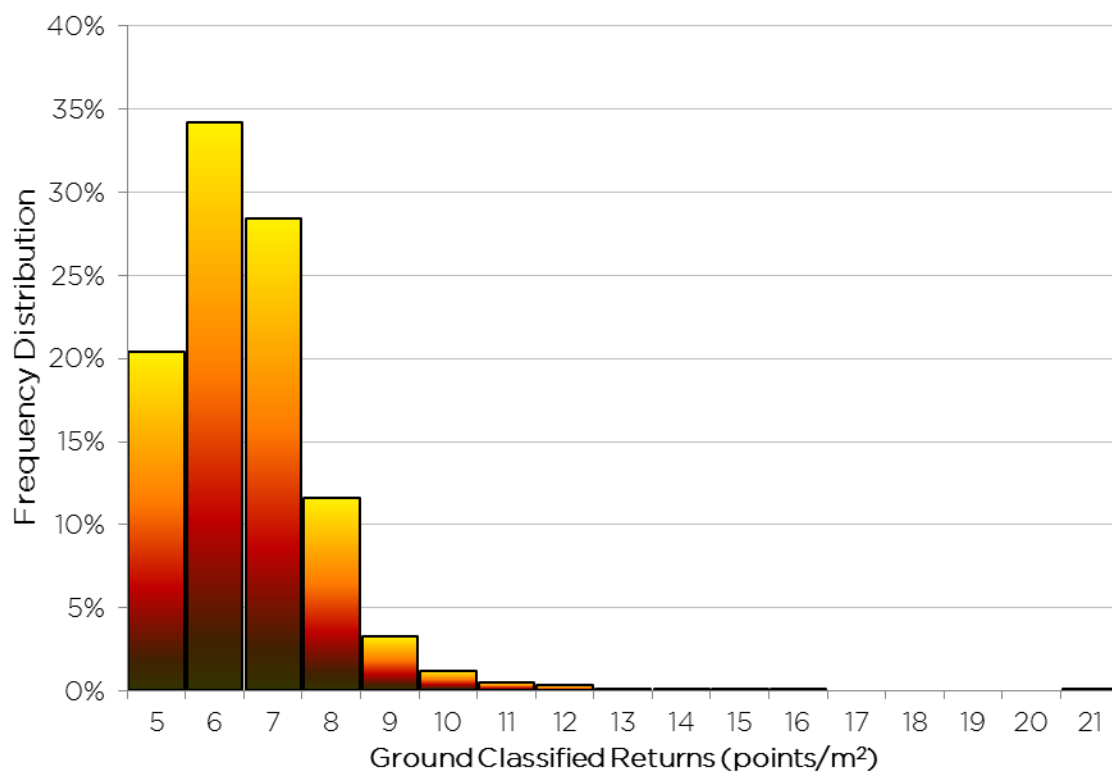


**Figure 5: Frequency distribution of ground return densities of the 1m gridded study area**

**Figure 6: Native density map for the Sunset Crater LiDAR site**



Native Point Density
points/meter $^2$

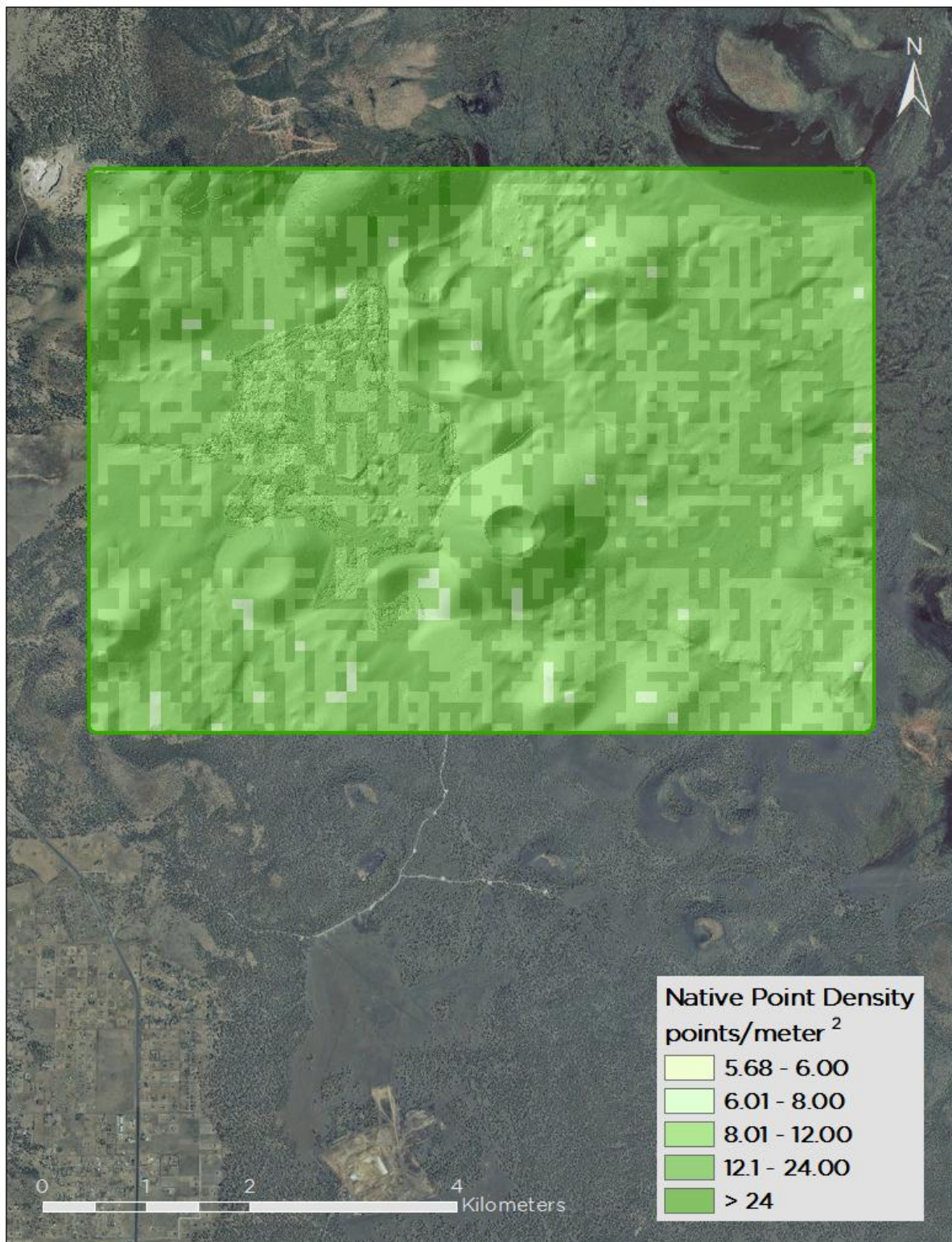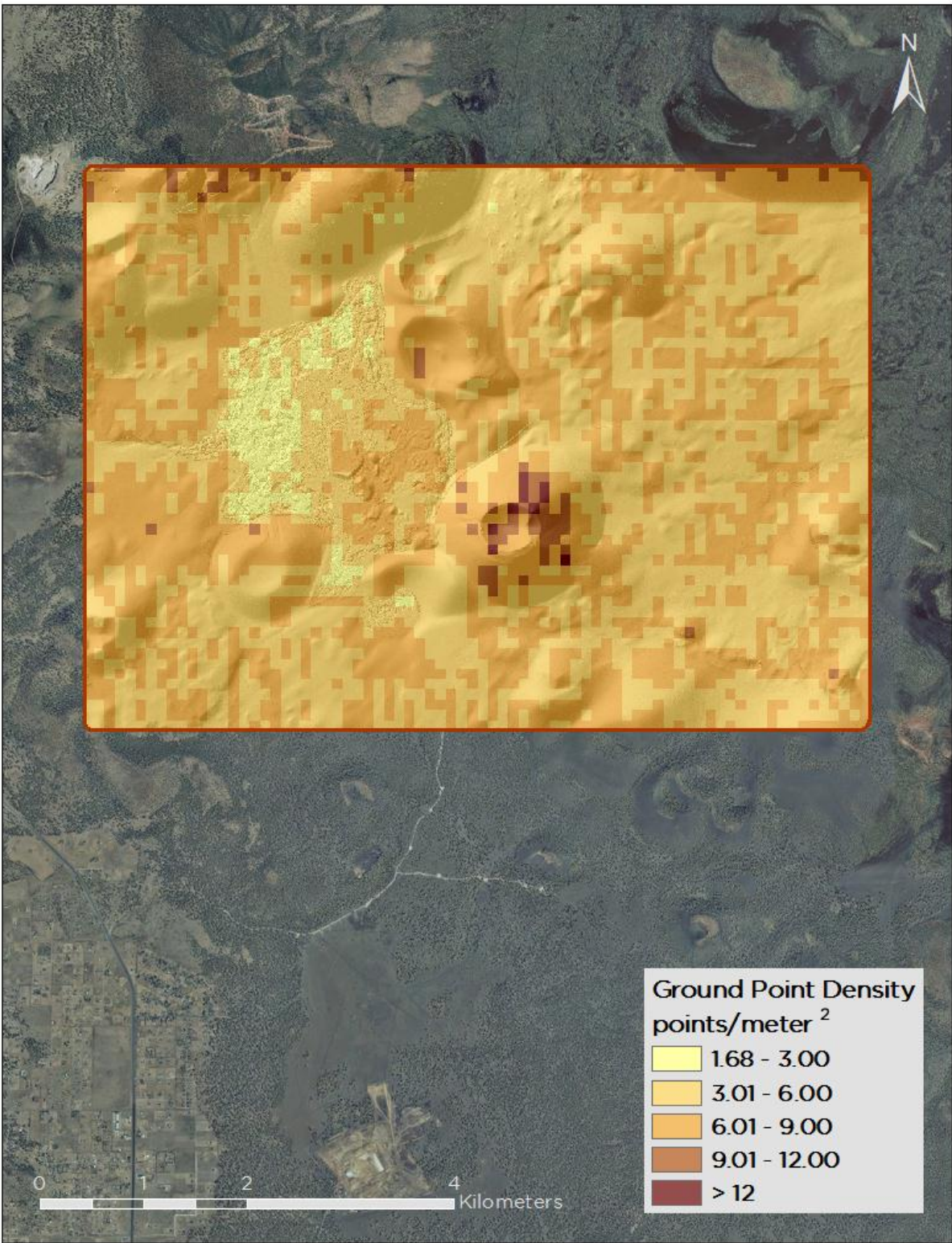| | |
|---|---|
| | 5.68 - 6.00 |
| | 6.01 - 8.00 |
| | 8.01 - 12.00 |
| | 12.1 - 24.00 |
| | > 24 |

**Figure 7: Ground density map for the Sunset Crater LiDAR site**

# LiDAR Accuracy Assessments

The accuracy of the LiDAR data collection can be described as the consistency of the data with external data sources (absolute accuracy) and the consistency of the dataset with itself (relative accuracy). See Appendix A for further information on sources of error.

## LiDAR Absolute Accuracy

Vertical absolute accuracy was primarily assessed from ground check point data collected on open, bare earth surfaces with level slope (<20°). Fundamental Vertical Accuracy (FVA) reporting is designed to meet guidelines presented in the National Standard for Spatial Data Accuracy (FGDC, 1998). FVA compares known RTK ground survey check points to the triangulated ground surface generated by the LiDAR points. FVA is a measure of the accuracy of LiDAR point data in open areas where the LiDAR system has a "very high probability" of measuring the ground surface and is evaluated at the 95% confidence interval (1.96 σ).

Absolute accuracy is described as the mean and standard deviation (sigma~σ) of divergence of the ground surface model from ground survey point coordinates. These statistics assume the error for x, y, and z is normally distributed; therefore, the skew and kurtosis of distributions are also considered when evaluating error statistics. For the Sunset Crater LiDAR survey, 665 hard surface RTK points were collected in total.

**Table 10: Absolute and relative accuracies**

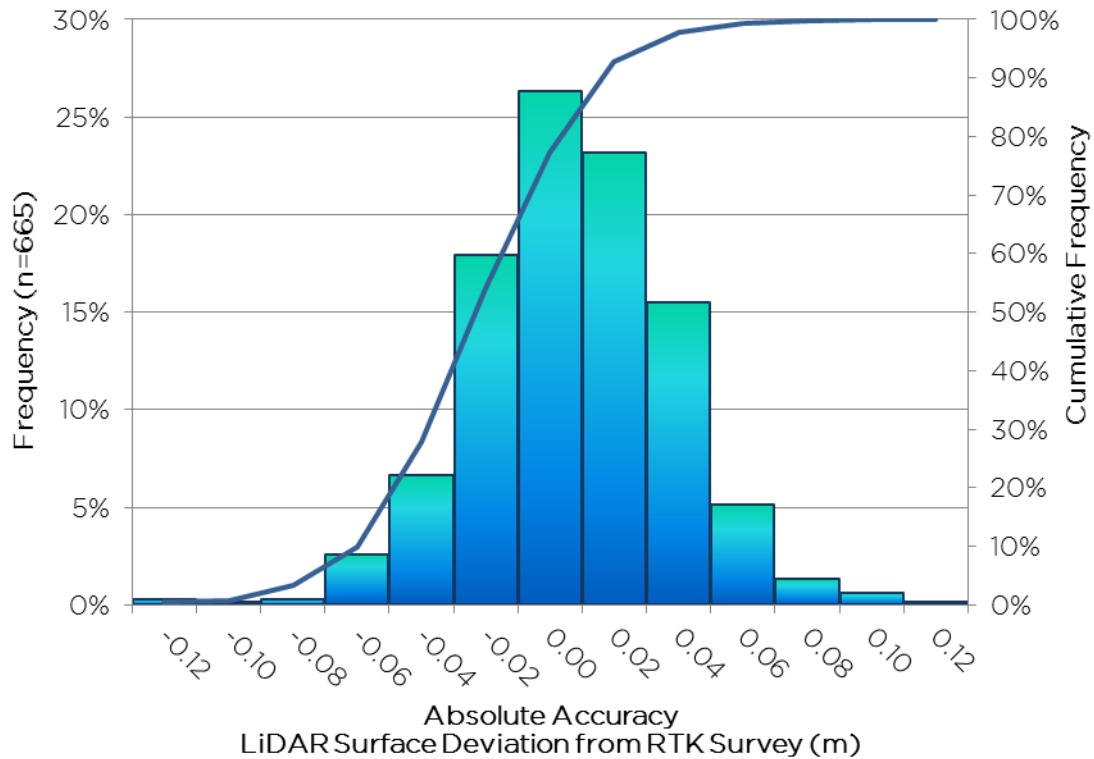|  | Absolute Accuracy | Relative Accuracy |
|---|---|---|
| Sample | 665 points | 81 surfaces |
| Average | -0.002 m | 0.033 m |
| Median | -0.002 m | 0.033 m |
| RMSE | 0.031 m | 0.033 m |
| 1σ | 0.031 m | 0.006 m |
| 2σ | 0.061 m | 0.012 m |

**Figure 8: Frequency histogram for LiDAR surface deviation from RTK values**

In addition to hard surface RTK, 148 land cover check points were taken throughout the entire study area. Land cover types and descriptions can be referenced in Table 5. Individual accuracies were calculated for each land-cover type to assess confidence in the LiDAR derived ground models across land-cover classes (Table 11).

**Table 11:  Land Cover statistics for the Sunset Crater AOI**

| Land Cover | Sample Size (n) | Mean Dz | 1 sigma (σ) | 1.96 sigma (σ) | RMSE |
|---|---|---|---|---|---|
| Montane grassland | 25 | 0.029 | 0.026 | 0.052 | 0.042 |
| Ponderosa Pine (contiguous) | 33 | 0.017 | 0.022 | 0.043 | 0.035 |
| Ponderosa Pine  (patchy) | 23 | 0.022 | 0.023 | 0.044 | 0.041 |
| Cinder and Basalt (sparse herbaceous) | 33 | -0.008 | 0.017 | 0.034 | 0.038 |
| Cinder terrain | 34 | 0.015 | 0.020 | 0.040 | 0.039 |

# LiDAR Relative Accuracy

Relative accuracy refers to the internal consistency of the data set as a whole—that is, the ability to place an object in the same location given multiple flight lines, GPS conditions, and aircraft attitudes. The relative accuracy is computed by comparing the ground surface model of each individual flight line with its neighbors in overlapping regions (Table 10, Figure 9). When the LiDAR system is well calibrated, the swath-to-swath divergence is low (<10cm). See Appendix B for operational measures that are taken to improve relative accuracy.
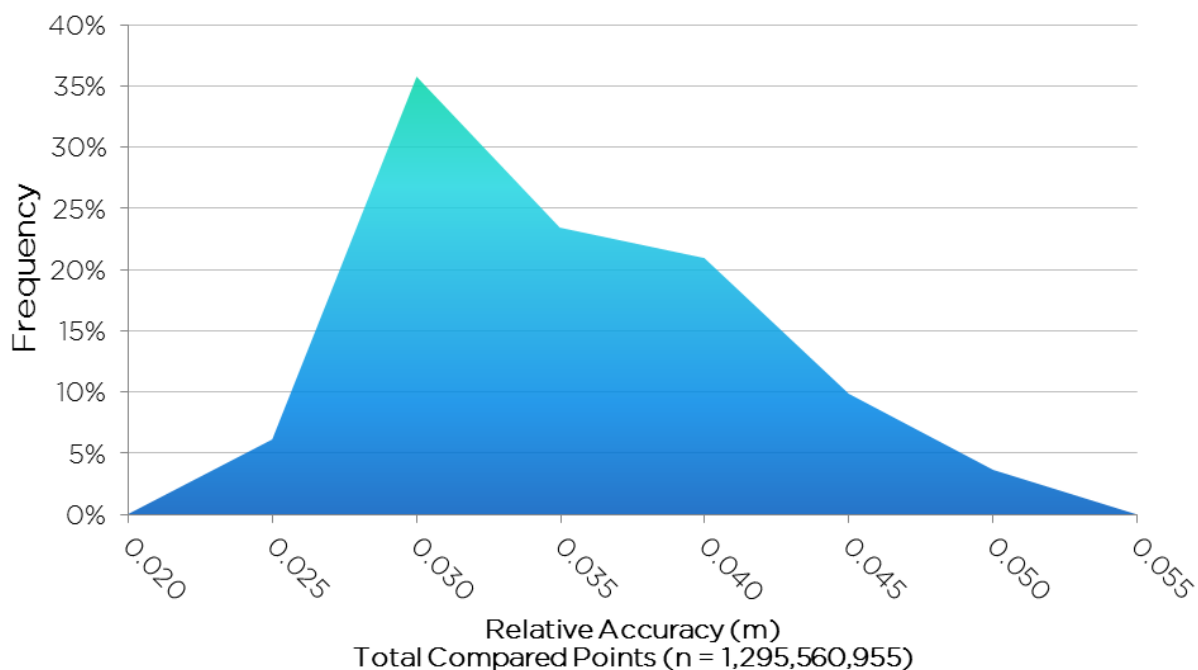


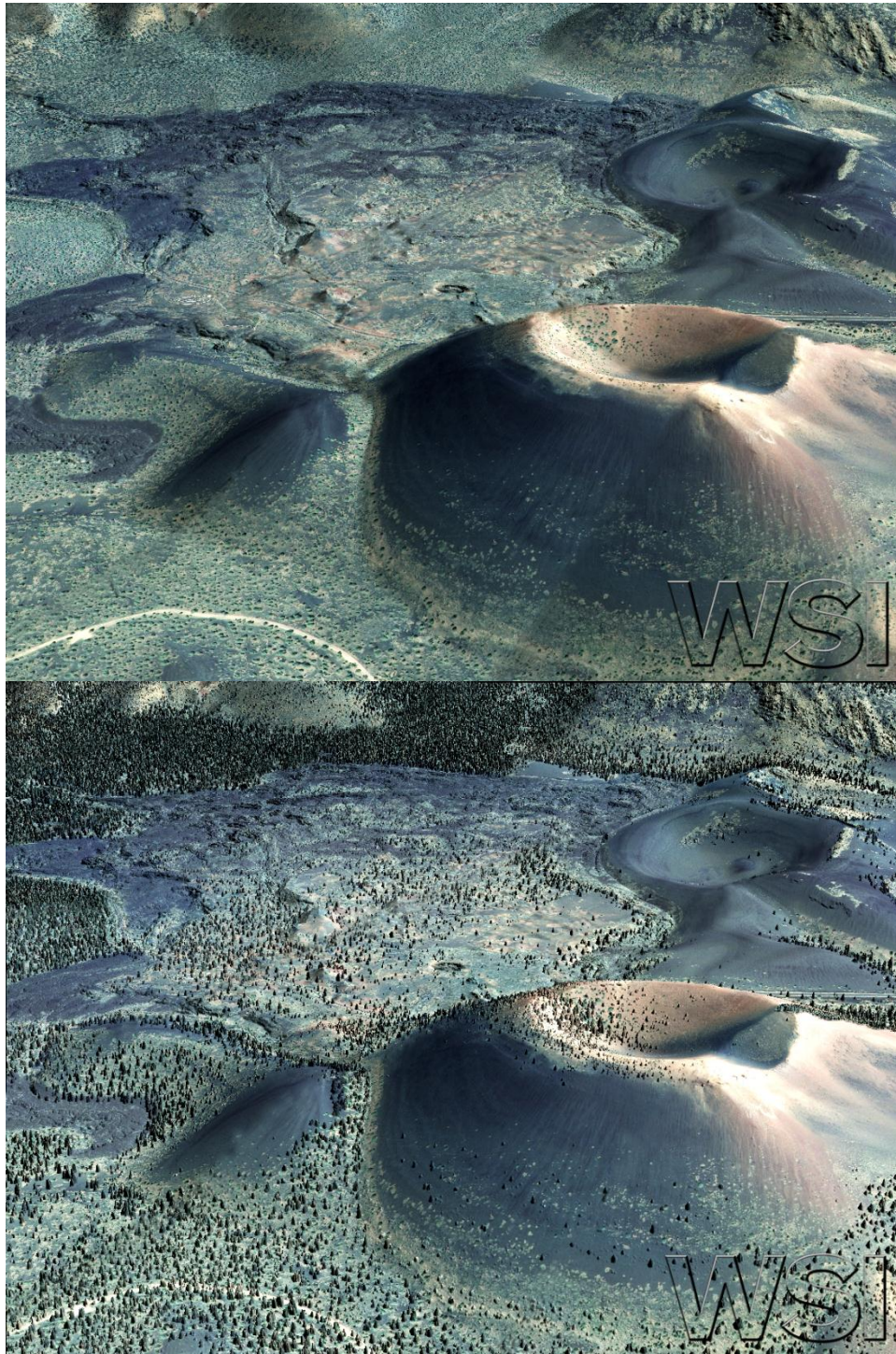**Figure 9: Frequency plot for relative accuracy between flight lines**

**Figure 10: View looking northwest over the Sunset Crater Volcano National Monument. Top image derived from bare-earth LiDAR points colored by 2010 NAIP imagery. Bottom image derived from all LiDAR points colored by 2010 NAIP imagery.**
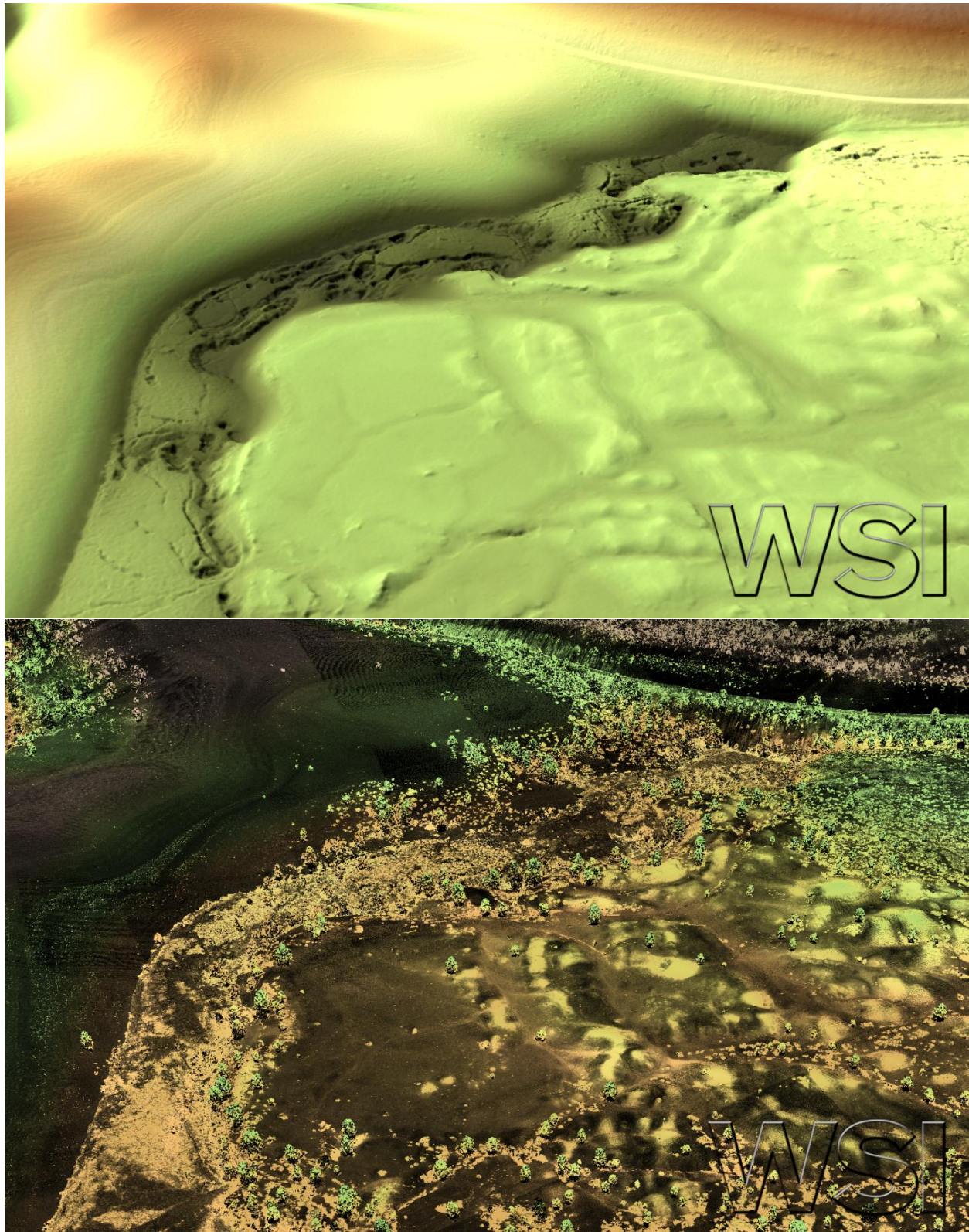
**Figure 11: The top image is a bare earth model colored by elevation, looking southeast at part of the Bonito lava flow at the base of the Sunset Crater. The bottom image is a 3D point cloud colored by height.**
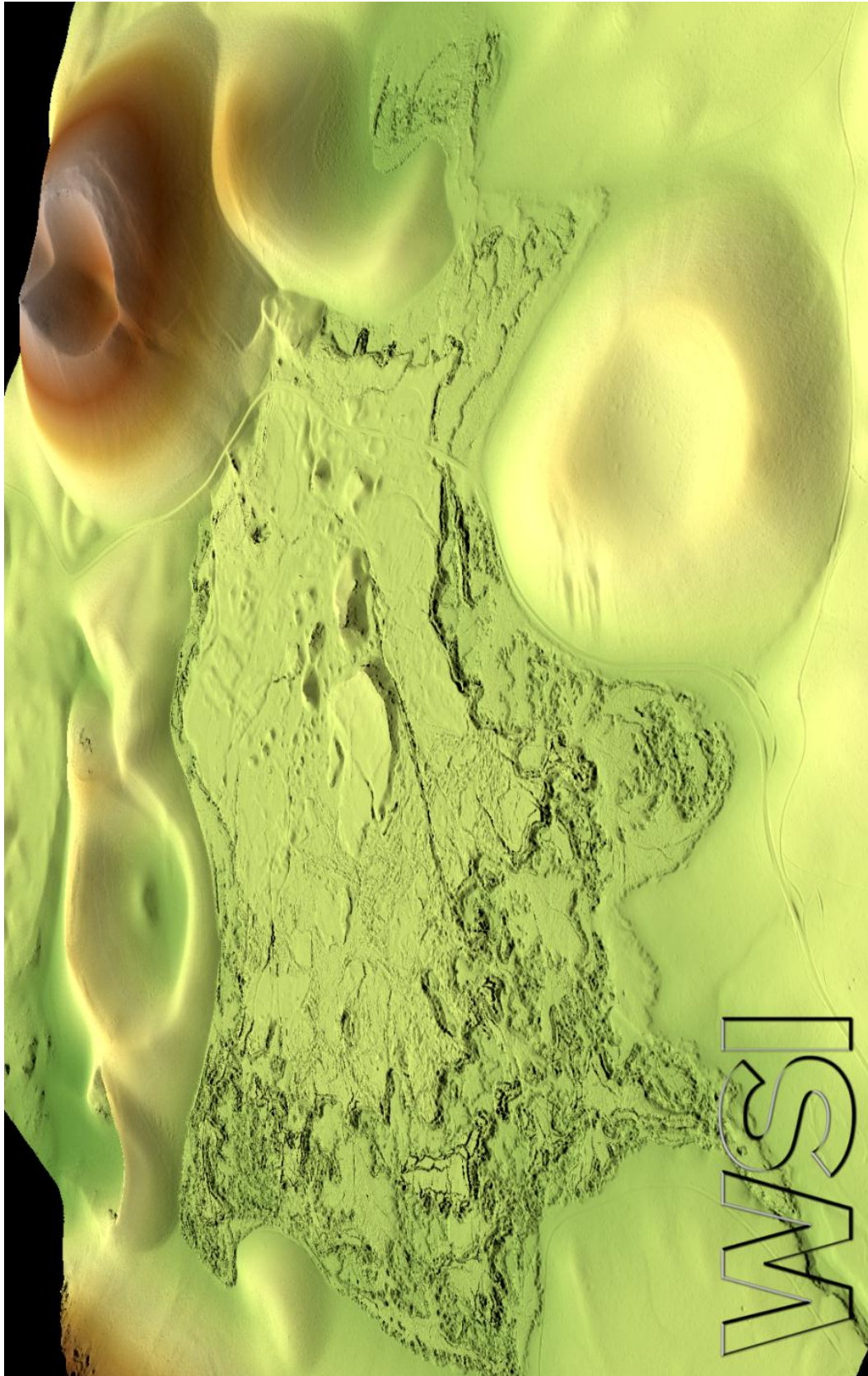
Figure 14: Bare-earth hillshade colored by elevation looking northeast at the Bonito lava flow and the Sunset and Lenox craters.

**1-sigma (σ) Absolute Deviation:**  Value for which the data are within one standard deviation (approximately 68th percentile) of a normally distributed data set.

**1.96-sigma (σ) Absolute Deviation:**  Value for which the data are within two standard deviations (approximately 95th percentile) of a normally distributed data set.

**Root Mean Square Error (RMSE):**  A statistic used to approximate the difference between real-world points and the LiDAR points. It is calculated by squaring all the values, then taking the average of the squares and taking the square root of the average.

**Pulse Rate (PR)**:  The rate at which laser pulses are emitted from the sensor; typically measured as thousands of pulses per second (kHz).

**Pulse Returns**:  For every laser pulse emitted, the Leica ALS 60 system can record *up to four* wave forms reflected back to the sensor. Portions of the wave form that return earliest are the highest element in multi-tiered surfaces such as vegetation. Portions of the wave form that return last are the lowest element in multi-tiered surfaces.

**Accuracy**:  The statistical comparison between known (surveyed) points and laser points. Typically measured as the standard deviation (sigma, σ) and root mean square error (RMSE).

**Intensity Values**:  The peak power ratio of the laser return to the emitted laser. It is a function of surface reflectivity.

**Data Density**:  A common measure of LiDAR resolution, measured as points per square meter.

**Spot Spacing**:  Also a measure of LiDAR resolution, measured as the average distance between laser points.

**Nadir**:  A single point or locus of points on the surface of the earth directly below a sensor as it progresses along its flight line.

**Scan Angle**:  The angle from nadir to the edge of the scan, measured in degrees. Laser point accuracy typically decreases as scan angles increase.

**Overlap**:  The area shared between flight lines, typically measured in percents; 100% overlap is essential to ensure complete coverage and reduce laser shadows.

**DTM / DEM**:  These often-interchanged terms refer to models made from laser points. The digital elevation model (DEM) refers to all surfaces, including bare ground and vegetation, while the digital terrain model (DTM) refers only to those points classified as ground.

**Real-Time Kinematic (RTK) Survey**:  GPS surveying is conducted with a GPS base station deployed over a known monument with a radio connection to a GPS rover. Both the base station and rover receive differential GPS data and the baseline correction is solved between the two. This type of ground survey is accurate to 1.5 cm or less.

### Laser Noise

For any given target, laser noise is the breadth of the data cloud per laser return (i.e., last, first, etc.). Lower intensity surfaces (roads, rooftops, still/calm water) experience higher laser noise. The laser noise range for this survey was approximately 0.02 meters.

### Absolute Accuracy

The vertical accuracy of LiDAR data is described as the mean and standard deviation (sigma σ) of divergence of LiDAR point coordinates from RTK ground survey point coordinates. To provide a sense of the model predictive power of the dataset, the root mean square error (RMSE) for vertical accuracy is also provided. These statistics assume the error distributions for x, y, and zs are normally distributed, thus we also consider the skew and kurtosis of distributions when evaluating error statistics.

### Relative Accuracy

Relative accuracy refers to the internal consistency of the data set - the ability to place a laser point in the same location over multiple flight lines, GPS conditions, and aircraft attitudes. Affected by system attitude offsets, scale, and GPS/IMU drift, internal consistency is measured as the divergence between points from different flight lines within an overlapping area. Divergence is most apparent when flight lines are opposing. When the LiDAR system is well calibrated, the line-to-line divergence is low (<10 cm).

### Relative Accuracy Calibration Methodology

Manual System Calibration:  Calibration procedures for each mission require solving geometric relationships that relate measured swath-to-swath deviations to misalignments of system attitude parameters. Corrected scale, pitch, roll and heading offsets were calculated and applied to resolve misalignments. The raw divergence between lines was computed after the manual calibration was completed and reported for each survey area.

Automated Attitude Calibration:  All data were tested and calibrated using TerraMatch automated sampling routines. Ground points were classified for each individual flight line and used for line-to-line testing. System misalignment offsets (pitch, roll and heading) and scale were solved for each individual mission and applied to respective mission datasets. The data from each mission were then blended when imported together to form the entire area of interest.

Automated Z Calibration:  Ground points per line were used to calculate the vertical divergence between lines caused by vertical GPS drift. Automated Z calibration was the final step employed for relative accuracy calibration.

LiDAR accuracy error sources and solutions:

| Type of Error | Source | Post Processing Solution |
|---|---|---|
| GPS (Static/Kinematic) | Long Base Lines | None |
| | Poor Satellite Constellation | None |
| | Poor Antenna Visibility | Reduce Visibility Mask |
| Relative Accuracy | Poor System Calibration | Recalibrate IMU and sensor offsets/settings |
| | Inaccurate System | None |
| Laser Noise | Poor Laser Timing | None |
| | Poor Laser Reception | None |
| | Poor Laser Power | None |
| | Irregular Laser Shape | None |

Operational measures taken to improve relative accuracy:

Low Flight Altitude:  Terrain following is employed to maintain a constant above ground level (AGL). Laser horizontal errors are a function of flight altitude above ground (i.e., ~ 1/3000th AGL flight altitude).

Focus Laser Power at narrow beam footprint:  A laser return must be received by the system above a power threshold to accurately record a measurement. The strength of the laser return is a function of laser emission power, laser footprint, flight altitude and the reflectivity of the target. While surface reflectivity cannot be controlled, laser power can be increased and low flight altitudes can be maintained.

Reduced Scan Angle:  Edge-of-scan data can become inaccurate. The scan angle was reduced to a maximum of 315$^o$ from nadir, creating a narrow swath width and greatly reducing laser shadows from trees and buildings.

Quality GPS:  Flights took place during optimal GPS conditions (e.g., 6 or more satellites and PDOP [Position Dilution of Precision] less than 3.0). Before each flight, the PDOP was determined for the survey day. During all flight times, a dual frequency DGPS base station recording at 1–second epochs was utilized and a maximum baseline length between the aircraft and the control points was less than 19 km (11.5 miles) at all times.

Ground Survey:  Ground survey point accuracy (i.e. <1.5 cm RMSE) occurs during optimal PDOP ranges and targets a minimal baseline distance of 4 miles between GPS rover and base. Robust statistics are, in part, a function of sample size (n) and distribution. Ground survey RTK points are distributed to the extent possible throughout multiple flight lines and across the survey area.

50% Side-Lap (100% Overlap):  Overlapping areas are optimized for relative accuracy testing. Laser shadowing is minimized to help increase target acquisition from multiple scan angles.

Ideally, with a 50% side-lap, the most nadir portion of one flight line coincides with the edge (least nadir) portion of overlapping flight lines. A minimum of 50% side-lap with terrain-followed acquisition prevents data gaps.

<u>Opposing Flight Lines</u>:  All overlapping flight lines are opposing. Pitch, roll and heading errors are amplified by a factor of two relative to the adjacent flight line(s), making misalignments easier to detect and resolve.